Dissecting the Suitability of DESI-MSI for Molecular Fingerprinting.

KRISHNA, Rohith, MILLARD, Georgia, BRADSHAW, Robert <http://orcid.org/0000-0003-1533-2166>, COLE, Laura <http://orcid.org/0000-0002-2538-6291> and FRANCESE, Simona <http://orcid.org/0000-0002-1381-1262>

Dissecting the suitability of DESI-MSI for Molecular Fingerprinting

[1]R. Krishna, [1]G. Millard, R. [1]Bradshaw, [1]L. Cole, and [1]S. Francese[*]

[1]Biomolecular Research Centre, Centre for Mass Spectrometry Imaging, Sheffield Hallam University, Sheffield S1 1WB, England, United Kingdom

* Corresponding author: s.francese@shu.ac.uk

Abstract

Since its inception in 2004, Desorption Electrospray Ionisation Mass Spectrometry (DESI MS) has seen a significant increase in its application to the pharmaceutical and clinical setting, supported by a steady improvement of the sensitivity, mass accuracy, mass resolution, spatial resolution and usability, as well as by the advantages offered by its ambient nature. However, in comparison to the rapid growth for tissue imaging, the uptake of DESI-MSI in fingerprint imaging has not grown a substantial body of knowledge, compared to MALDI-MSI. In this work, we set off to dissect the application of DESI-MSI to fingerprint imaging to explore both the advantages and the potential challenges that might have slowed down the uptake, taking stock from our previous work and that of others in this area. During this endeavour we have highlighted advantages but also discovered that, under a range of optimised operating conditions, fingerprint imaging by DESI-MSI is affected by a delocalisation phenomenon which we termed "the bleeding effect". This phenomenon shows to be specific to fingerprints, as sample type, as opposed to biological tissues, and may be one of the contributing factors to a seemingly slower uptake of this technique in molecular fingerprinting. Therefore, a description of the observed effect, how to minimise it, and its implications in operational work are discussed.

Keywords: DESI-MSI, fingerprints, imaging, forensics

Introduction

Whilst still a niche application area for mass spectrometry imaging (MSI), (forensic) molecular fingerprinting is emerging as a very informative new discipline in the forensic science domain. The approach enables the provision of biometric information through the reconstruction of the fingerprint ridge pattern, via the visualisation of molecules present on the fingerprint ridges. As molecular information can be recovered, molecular fingerprinting via MSI can also serve as means to undertake *"chemical criminal profiling"* [1], that is, the tentative provision of the individual's personal information, such as lifestyle [2,3], use of medication [2], sex [4,5], pathological states [6]. When forensically relevant, chemical information is mapped onto the ridge pattern; the identity of the owner of the mark can be therefore linked to contextual information on the individual and/or the crime scene and the circumstances of the crime [7-9]. A few MSI techniques, including Matrix Assisted Laser Desorption Ionisation MSI (MALDI-MSI), Secondary Ion Mass Spectrometry MSI (SIMS MSI), Laser Desorption Ionisation MSI (LDI MSI), Desorption Electrospray Ionisation MSI (DESI-MSI) and Surface Assisted Laser Desorption MSI (SALDI MSI) [10] have been published providing varying degrees of quality of biometric and chemical information, body of knowledge generated. They are characterised by different technology readiness level (TRL), occasionally only focussing on chemical profiling rather than on the biometric information.

Firstly published in 2009 for molecular fingerprinting [11], MALDI-MSI has accrued the highest number of publications, built the largest body of knowledge, and acquired the highest TRL, which, depending on the type of application, can be up to 9 [12]; this is reflected by the inclusion of Molecular Fingerprinting by MALDI-MSI in the Fingermark Visualisation Manual (FVM) edited by the Home Office, UK, as Category C in 2014 [13] and subsequently promoted in the FVM (edited by the Home Office and the Dstl, UK) as Category B in 2022 [14]. In the context of molecular fingerprinting, SIMS Imaging is complementary to MALDI-MSI in terms of capabilities and molecular targets. However, though its submicron spatial resolution is still superior to that of MALDI-MSI (which can achieve, at best, 5 µm pixel size), this is not needed for molecular fingerprinting; here this level of spatial resolution is unnecessary and only significantly increases acquisition times, operationally non-ideal when fast answers are needed in major crimes. SIMS however, has also generated an appreciable body of knowledge which warranted its inclusion in the FVM as Category C technique in 2014, though the technique is less mature and more destructive than MALDI-MSI and has not yet progressed to Category B.

Interestingly, the first scientific paper describing molecular fingerprinting using DESI-MSI was published in 2008 and was the first MSI technique used for this type of application [15]. At that point, DESI MS and MSI had only been around 4 years [16]. Since 2004, biomedical and biomarker-based applications using DESI-MSI have steadily grown due to DESI's ambient ionisation conditions allowing for acquisitions to be made at atmospheric pressure and not requiring the use of a chemical matrix (unlike vacuum/ambient MALDI-MSI). Due largely to the specimens being analysed in their native state, and also to very recent technological

improvements enabling higher mass accuracy and spatial resolution, DESI-MSI has seen a rapid surge in its applications particularly in cancer and biomedical research, and even being used as an intra-operative technique, enabling the real time assessment of tumour margins [17-19].

However, whilst molecular fingerprinting via MALDI-MSI is still very much pursued by the wider community and has been used in Police casework [3], the application of DESI-MSI in this area has been slower. The authors have undertaken a literature search using Pubmed, Web of Science, Google Scholar and Scopus to recover peer reviewed publications reporting on the application of both MALDI-MSI and DESI-MSI to molecular fingerprinting between 2008 and 2025. Review articles and articles not applying the imaging modality and hence not providing molecular images of fingerprints have been excluded. In a handful of cases, both DESI-MSI and MALDI-MSI had been employed in the same published research, and these publications have been included in both the MALDI-MSI and DESI-MSI count. The searches returned a total of 16 publications for DESI-MSI and 46 for MALDI-MSI; the breakdown per year of the number of publications on fingerprint imaging by MALDI-MSI is significantly higher than DESI-MSI across the period investigated (Fig. S1).

However, an additional literature search shows that this trend is mirrored in the total number of MALDI-MSI papers versus DESI-MSI papers (covering all other applications).

Within publications underpinning Fig. S1, DESI-MSI has largely replicated MALDI-MSI applications already published covering simple latent fingermark imaging [20-24], condom contaminated fingermark imaging [25-26], time since deposition [27], drug imaging in fingerprints [23, 28-29] and determination of sex [30] although the latter suffers from insufficient amount of donors to draw conclusions, with some of publications on compatibility with three fingerprint enhancement techniques namely Oil Red O [31], cyanoacrylate fuming [26] and white powder [24].

The latter original paper [24] represented the first time that DESI-MSI was applied to fingerprint on gelatine lifters, rather than tape lifts, and the first publication in which fingermark images presented clear and quality ridge detail. Gelatine lifters are unsuitable for vacuum MALDI-MSI due to their high content in water and hence, DESI-MSI would be a valid alternative to MALDI-MSI in the presence of fingerprint recovered by gelatine lifters. However, an interesting observation was made by Frisch et al [24] in that, for each of the 3 consecutive DESI-MSI runs they conducted on the fingerprint on the gelatine lifter: *"the spray of solvent onto the surface of the lifter caused the gelatine layer to be etched, and the fingermark to be gradually washed off the gelatine support".* Even though they labelled this effect as minimal, this observation supported and partly motivated the experimental work we presented here.

DESI is a newer technique than MALDI for MSI and it may be possible that the only recent more significant commercial development of DESI in MSI compared to MALDI, could have also impacted the uptake of the fingerprinting imaging application. Within the research

work described in this paper, the authors have intended to explore whether there may be any, technological challenges, contributing to the smaller body of knowledge generated. Here we explore both DESI MSI merits and limitations within molecular fingerprinting. This work was also prompted by recent observations in our laboratory in applying a multi-modal imaging workflow for the detection of antipsychotics and date rape drugs, some of which has been recently published [28]. In that study we observed the formation of a "halo" in DESI-MSI fingerprint images and/or loss of clarity and definition of the ridge detail both outside and inside the fingerprint, consistent with a phenomenon that the authors named in the present study "molecular bleeding". Having optimised the instrumental and analytical acquisition parameters on the state-of-the-art DESI ionisation source, the authors suggest that molecular bleeding within fingerprint imaging by DESI-MSI is surface-and molecule-dependant, and in those cases and *under the conditions explored*, unavoidable.
This phenomenon appears to be fingerprint-specific (intended as sample type and as opposed to tissue sections) due to it being a thin layer of sweat compared to, for example, tissue sections where molecules on the surface benefit of a greater resistance to migration, potentially caused by electrospraying the solvent in DESI. Instances of reduced effect in molecular fingerprinting have been identified, and recommendations have been provided in the context of operational casework.

Materials and Methods

Materials

Ultra-pure methanol (MeOH) and formic acid (FA), used for DESI analysis, were purchased from ROMIL Ltd. (Cambridge, UK). The Milli-Q water was obtained from an in-house Millipore water purification system (Merck KGaA, Darmstadt, Germany). The analytical standards of diazepam (DIA), alprazolam (ALP), and flunitrazepam (FLU) were purchased from Merck Life Science (Gillingham, UK). Double-sided conductive carbon tape was purchased from TAAB (Aldermaston, UK). Glass microscope slides (75 mm × 25 mm) were sourced from Fisher Scientific (Leicestershire, UK), Aluminum powder for fingerprint development and lifting tape were purchased by SceneSafe (Burnham-on-Crouch, England) and gelatine lifters were kindly donated by Dr Anne Therese Sletta, Forensic and ID department Fingerprint unit, NCIS, Norway.

Instrumentation

Optical co-axial and optical variable device (OVD) imaging in the visible range (400-800 nm) of both fingerprints and liver sections was conducted using a VSC 4CX system (Foster & Freeman, Worcestershire, UK). Fresh frozen liver samples were cryo-sectioned with a Leica CM3050 S Cryostat (Leica Biosystems, Nussloch, Germany). DESI-MSI analysis was performed on a SELECT SERIES Cyclic IMS- (cIMS) mass spectrometer equipped with a DESI XS source (Waters Corporation, Wilmslow, UK).

Methods

Mass Spectrometry data acquisition and Data Processing

All data were acquired in the mass range *m/z* 50 –1,200 in positive ionization and Time-of-Flight (TOF) sensitivity mode. In optimised conditions, the DESI solvent consisted of (95:5 methanol/water with 0.1% formic acid (v/v) and was spiked with leucine enkephalin (100 pg/µL) for continuous lock mass correction. Quadrupole profile and transfer RF parameters were adapted from Krishna et al. [32] for small molecule analysis; the quadrupole RF profile was manually set at *m/z* values of 250, 300, and 400 whilst the transfer RF was set to 150 V. Prior to each analysis, the instrument was calibrated using polyalanine. Mass spectrometry data were acquired using MassLynx™ (v4.2 SCN1016), and Quartz (v2.12.1).
The DESI XS source was set up for imaging experiments using the previously optimised method by the authors [28]. A summary of the DESI XS source parameters for imaging acquisitions is provided in Table 1.
Mass spectra were processed directly in Masslynx v4.2. MSI experiments were set up using Quartz. All the DESI-cIMS imaging experiments were processed and visualised using High-Definition Imaging (HDI) software v1.8 (Waters Corporation, Wilmslow UK) with the following settings: V-mode with a mass resolution of 60,000, *m/z* window of <0.01 amu, for m/z 50-500 Da and the number of most intense peaks set to 1000. All the images were Total Ion Count (TIC) and normalised unless specified otherwise.

Table 1. The DESI parameters and the optimised values. (a) The HTL temperature is set to 250°C only for imaging on gelatine lifted fingerprints [23]

Parameter	**Optimised Value**
Source capillary voltage	0.7 kV
Sampling cone voltage	40 V
Source temperature	120°C
HTL temperature	100°C, 250°C (a)
Solvent flow rate	1 µL/min
API gas pressure	0.08 mPa
Stage rate	450 µm/s
Pixel size	50 µm x 50 µm
Sprayer angle (α)	72°

Relevant regions of interest (ROI) were exported to MassLynx™ v4.2 software for analysis of the mass spectra. Multivariate analysis (MVA) was performed using Metaboanalyst v6.0 [33]. Principal component analysis (PCA) was performed by selecting, regions of interest (ROIs) using HDI v1.8 and exported as MVA file with TIC normalisation applied.

Fingerprint sample preparation for DESI-MSI analysis

All the fingerprints were deposited by the same one donor in accordance with the ethics approved by Sheffield Hallam University, UK (ER60882966). Fingerprints were deposited in triplicates except for the biological tissue-fingerprint comparative analysis. DESI imaging was primarily carried out on natural fingerprints (i.e. generated without any prior enrichment or washing of the fingertips) deposited onto microscope slides, which were then secured to the DESI stage. Where groomed prints were used, it is specified in the text. Diazepam-, alprazolam- and flunitrazepam-contaminated fingerprints were prepared adapting the method from Groeneveld et al. [34]. Briefly, 50 µL methanolic solutions of each drug at concentrations of 1 mg/mL was spotted onto a clean glass slide. Upon solvent evaporation in ambient conditions, a fingertip was thoroughly swiped across the dried residue. The drug-contaminated fingertip was then pressed against a clean glass slide to produce a drug-contaminated fingerprint. Drug-contaminated fingerprints were also generated on four different surfaces of deposition namely glass, paper, lifting tape and gelatine lifters. The latter 3 substrates were secured to glass slides using double-sided conductive carbon tape whilst the glass slide was analysed directly. For the analysis of lifted prints, natural fingerprints were first deposited on a black tile, developed with aluminum powder, and subsequently lifted.

Computational Fluid Mechanics of Fingerprint Imaging by DESI-MSI

A 2D simulation scripted in Python and designed to be run in a Jupyter Notebook environment via Anaconda Navigator, was developed to model the fluid dynamics of the electrosprayed solvent on fingerprint, thus simulating aspects of Desorption Electrospray Ionization (DESI) mass spectrometry. The source code for the simulation is openly accessible on a GitHub repository (https://github.com/thealchemist26/desi-solvent-simulator) along with the user manual and documentation. The computational fluid mechanics (CFM) were simulated using the Lattice Boltzmann Method (LBM) [35], specifically the two-dimensional nine-velocity (D2Q9) model on a square grid. The evolution of particle distribution functions for the solvent particle was governed by the Lattice Boltzmann equation with the Bhatnagar-Gross-Krook (BGK) approximation [36], the kinematic viscosity (ν) of the simulated fluid was directly related to the relaxation time (τ), with a stable simulation requiring $\tau > 0.5$. The approximate kinematic viscosity (ν) and corresponding relaxation time (τ) values for various solvents and the DESI solvent system (methanol:water, 95:5) is reported in the Github documentation. Solid boundaries (fingerprint ridges) were treated as no-slip surfaces where the macroscopic velocity was explicitly set to zero. A certain roughness factor was included to the ridges to simulate real life irregularities in fingerprint ridges by adding and removing pixels at the ridge outer edge to create jaggedness. A gaussian spray velocity profile was imposed at the left boundary to simulate the DESI spray source, while a simple extrapolation boundary condition allowed fluid to exit the domain at the right boundary to prevent any backflow simulations. This simulation does not simulate

analyte transport by the solvent and only shows the fluid flow of the solvent system across a fingerprint sample.

The CFM script (DESI Solvent Simulator) works through a graphical user interface (GUI) to enable an easier parameter DESI parameter control. The sample characteristics and DESI parameters such as fingerprint ridge type (parallel ridge, whorl, arch etc), sample rotation angle, DESI sprayer angle (α), tip distance (d1), spray width, spray profile, and fluid relaxation time (τ) can be manually set to match the experimental parameters closely. In this study's experiments, the parallel, and whorl type ridges were studied; sample rotation of -32 degrees was used for the parallel ridges, a spray angle of 72°, tip distance was set to 1, spray width of 1 in gaussian profile and the relaxation time was set to 1.00 to approximately match the experimental solvent system conditions. The theoretical outputs of this fluid simulation were subsequently compared to the those of the fingerprint imaging experiments. The schematics and the GUI is presented in the supplementary Figure S2.

Contextual DESI Imaging analysis of Fingerprints and Biological Tissue (Liver)

Fresh frozen lamb liver was cryosectioned to 10 µm sections and thaw-mounted onto glass microscope slides. The tissue sections were immediately dried under a stream of nitrogen, vacuum-packed, and stored at -80 °C until analysis. To investigate potential variation in DESI imaging performance, a natural fingerprint was deposited onto the same slide, spatially above the liver section. This allowed both the fingerprint and the tissue to be analyzed in a single region DESI-MSI experiment.

Results and Discussion

The application of DESI-MSI to tissue imaging for biomedical application has grown significantly since its inception. With reference to forensic analysis, DESI has been successfully applied to ink analysis [37, 38], to the detection of whisky counterfeiting [39] and to condom lubricant classification [25,26] as well as being investigated in molecular fingerprinting [15, 23, 24-27]. Particularly, but not exclusively in the latter application, the ambient conditions and the minimal, or no sample preparation make the technique highly attractive in an operational environment. For this reason, it is important to explore the advantages and, if any, the limitations that may exist for the technique in this specific application, in order to address them and realise the DESI-MSI benefits in this area of application. The DESI-MSI images obtained in recent work incorporating DESI-MSI in a multimodal approach for antipsychotic drug detection [28] have further triggered the need to investigate the suitability of DESI-MSI, in the light of potentially implementing this technique in forensic operational setting, complementing fingerprint analysis by MALDI-MSI at the molecular level. After exploring different variables and parameters such as solvent and solvent composition/flow rate, sprayer angle/height, HTL temperature and API gas

pressure, in the present study, we investigated molecular fingerprinting via DESI-MSI in terms of the quality of the biometric ridge detail it provides. To this effect, the small molecule mass range 50-1,200 was investigated; its effectiveness in mapping drugs in fingerprints (as one of the representative forensic opportunities) was also explored. For this initial study, one donor only has been employed. This may be seen as a potential limitation, as for somewhat similar studies, a range of donors, bearing chemical diversity, is usually ideal. However, for this particular and initial study, we considered appropriate to the scope to rely on the chemical diversity within the same donor's fingerprint (and their fingerprints employed across the duration of the study) as it contains already diverse molecular classes, at least metabolites, lipids, and likely contaminants, in the mass range examined. Additionally, the use of the same one donor has allowed for better understanding of the effect of the change of a significant number of variables within the DESI parameters.

Finally, in these endeavour we also evaluated the physical effects of the solvent spray on the sample, through both experimental methods and fluid dynamics modelling. Two fingerprint orientations, with respect to the direction of DESI sampling direction, namely parallel and perpendicular were also investigated (Fig. S3).

Furthermore, DESI-MSI performance in molecular fingerprinting was investigated on four representative and forensically relevant surfaces of deposition.

DESI MS Fingerprint Imaging

Following on from the optimisation carried out in previous work [28], here we have further explored the impact of a number of variables on the quality of the resulting DESI MS images with the aim of reducing analyte diffusion, with a sample of these optimisation experiments reported in Supporting Information. In particular we have trialled/optimised: (i) three solvent systems namely 95:5 methanol:water, 100% methanol and 100% acetonitrile; (ii) two different flow rates (1 and 2 µL/min) (data not shown); the flow rates trialled are compatible with our current configuration and capabilities, considering that in previous research, attempts to increase the flow rate to 3 µL/min resulted in analyte delocalisation [22,23,26,28-30]; (iii) DESI sprayer angles (62°-78° in increments of 2°) (Fig S4), with angles lower than 62° generating progressively worse fingerprint image quality; (iv) different DESI sprayer head heights (data not shown); and (v) DESI API gas pressure from 0.08 mPa (default) to 0.04 mPa in increments of 0.01 mPa (Fig S5); (v) stage speed, optimised between 200-600 µm/s in 50 µm/s increments (data not shown); (v) HTL temperature from 100°C to 200°C in 20°C increments (Fig S6); furthermore a fingermark on an aluminium slide was enhanced with aluminium powder, tape lifted and imaged using an HTL temperature of 30°C which was the temperature setting recently reported by Rajs et al [27]; this particular experiment yielded no molecular images. The experimental exploration of all of these conditions has resulted in the adoption of the parameters reported in Section 2.4.1 for the study presented here. The conditions that limited bleeding the most are reported in Table 1. Under Table 1 optimised conditions, a latent natural fingerprint was deposited on a glass

slide and imaged by DESI-MSI under optimised source capillary and cone voltages. Ions detected across the entire mass range which provided fingermark images of varying quality were investigated and observed to all exhibit the same phenomenon to varying extents; owing to the impossibility to show mass images for each, within this study, ion images of representative quality were selected to support the observations. Accordingly, two fingerprint ion images at *m/z* 589.4280, and *m/z* 549.4127 have been selected and graded 2 and 4 respectively, (from lower to higher quality) - according to the scheme by Bandey et al [40] - and shown in Fig 1.

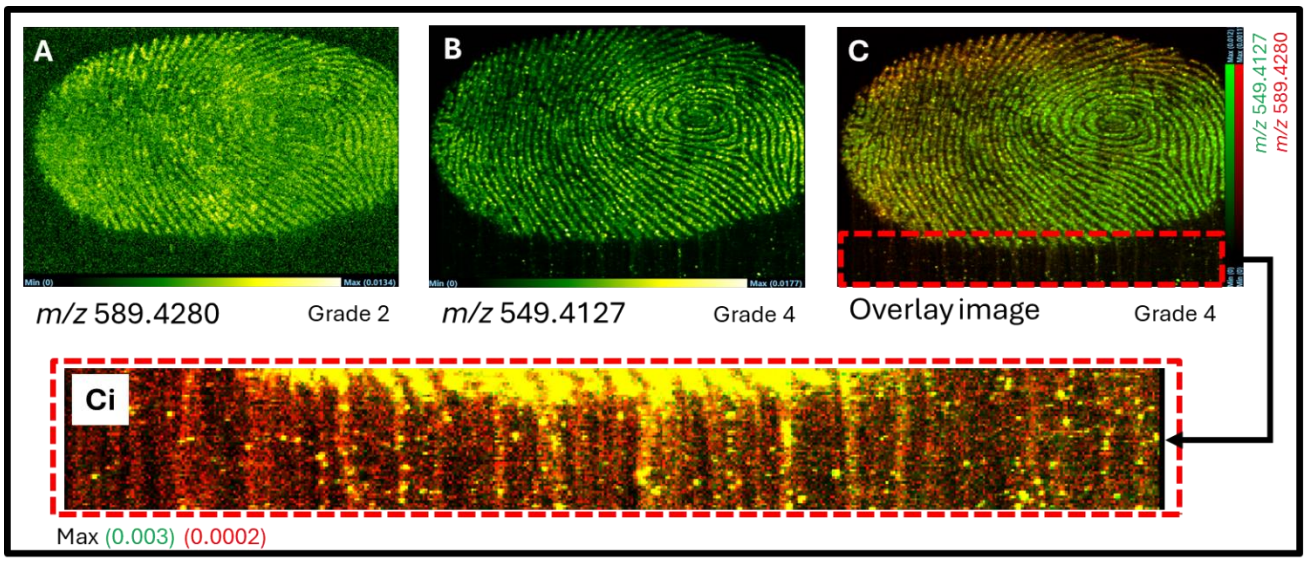

Figure 1. DESI-MSI a of latent natural fingerprint showing ion images of varying quality, graded according to Bandey et al [37] at (A) *m/z* 589.4280 grade 2, (B) *m/z* 549.4127 grade 4, and an overlayed image (C) (grade 4) with a zoom image of C highlighted in a red framed box. Panel (Ci) shows the highlighted area from (C) with adjusted intensity threshold. Imaging data are normalised by TIC. Pixel size at 50 µm. Within the elected grading system [37], grade 0 = No evidence of print; grade 1 = Some evidence of contact but no ridge detail present; grade 2= Less than 1/3 of print showing clear ridge detail; 3 = Between 1/3 and 2/3 of print showing clear ridge detail; 4 = Over 2/3 of the print showing clear ridge detail.

The images of the individual ions and distribution is shown in panels A and B and their overlay is reported in Fig 1C. It is clear that, especially from Fig 1B and C, most of the molecular signature is still located on the ridges, thus permitting a molecular reconstruction of the fingerprint. However, all images show a certain degree of analyte migration from the ridges into the adjacent furrows and further into the space outside the fingerprint sample, with this observation being clearer in the zoomed panel (Ci); the drier 100% methanol solvent did not alleviate molecular bleeding (data not shown); similarly, after the replacement of the methanol-based solvent with acetonitrile, analytes migration is still observed (Fig S7). A subsequent experiment confirmed delocalisation as another DESI-MSI acquisition was performed by selecting an area extending beyond the boundary of the fingerprint and revealing the significant presence of analyte signal in areas outside the

region where the print was initially deposited (data not shown). These observations suggest solvent-mediated transport of the analytes away from the ridges as observed in Figure 2 for the ion at *m/z* 509.3354 (Fig 2A); this ion image was selected as representative of those ions yielding images of intermediate ridge coverage (grade 2-3) and with no apparent delocalisation, which though becomes evident when increasing the image brightness by reducing the max intensity scale by 0.023 units; this image reveals a clear diffusion of the analyte away from the fingerprint and whilst some areas of the fingerprint gain quality, others lose biometric information.

We termed this migration/delocalisation phenomenon as the "bleeding effect". Figure 2E and 2F clearly show the presence of the ion at *m/z* 509.3354, representative of this effect, at notable intensity count and quantifiable signal-to noise (S/N) from regions of interest selected within the fingerprint (S/N 320) and in the bleeding area (S/N 12), respectively. The S/N was calculated from the extracted ion chromatogram (XIC) for the ion at *m/z* 509.3354. The accurate identification of this and other analytes detected and imaged across the entire mass range is unimportant here because the provision of biometric information is standalone intelligence that can be detached from the identity of the analyte that has generated it. However, we have explored the relationship between differential delocalisation extent and the chemical nature of the analyte in subsequent experiments using drug standards as later described in this paper.

Given that latent fingerprints have high molecular complexity [41] and consist of a thin layer (approx. 0.1 µm in height) of sweat [42], the DESI solvent can readily dissolve and mobilize susceptible analytes to migrate across not just one but multiple ridges and localize additionally in the furrows; the extent of the delocalisation is based on both their solubility in the solvent and affinity for the ridge chemical matrix. The ridge-and-furrow topography of a fingerprint then directs this flow, causing the solvent carrying the susceptible analytes to migrate outside the original deposition area.

These observations prompted the investigation of how this effect is influenced by the fingerprint's spatial orientation relative to the DESI sampling direction. To support this experimental work from a theoretical standpoint, the solvent electrospray and the subsequent analyte migration were also modelled using a simple 2D computational fluid dynamics (CFD) script.

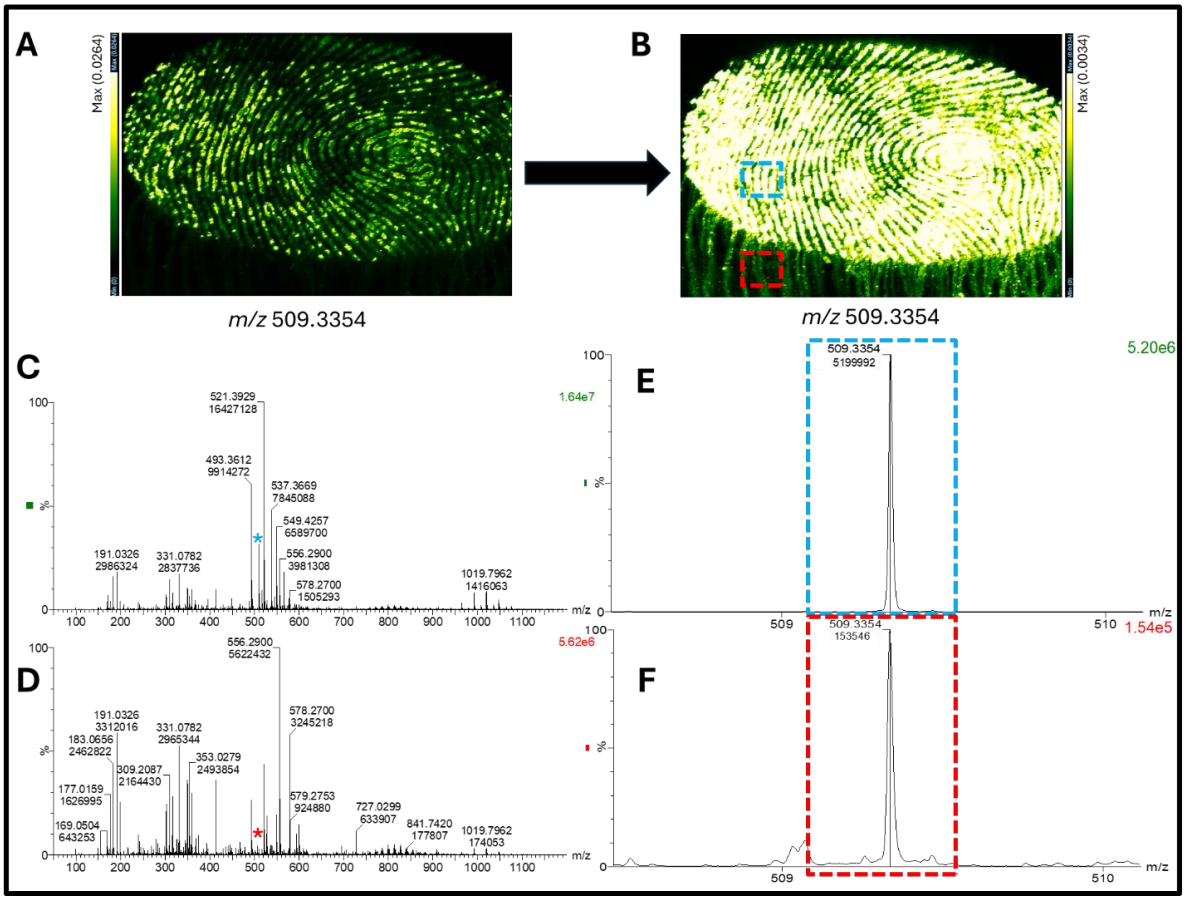

Figure 2. DESI MS images of a latent fingerprint. (A) and (B) are the ion images at *m/z* 509.3354, with (B) generated through increased brightness by reducing the max intensity scale by 0.023 units. (C) and (D) show the extracted mass spectra from a region of interest inside the fingerprint area (blue square in B) and outside the fingerprint area (red square in B) containing the same number of pixels. (Ci) and (Di) are zoomed in spectra displaying the ion at *m/z* 509.3354 from these ROIs and confirming presence of this representative species, outside the fingerprint area. Images are normalised by TIC. Pixel size at 50 µm.

Effect of Fingerprint Orientation

Our initial experiments with fingerprints deposited parallel to the sampling direction suggested that the "bleeding effect" resulted from analyte migration, with analytes channelled in the furrows. To test this hypothesis, fingerprints perpendicular to the sampling direction were also investigated to compare both the resulting image quality and pattern/appearance of the fingerprint resulting from the bleeding effect. The 2D computational fluid dynamics (CFD) modelling provided further insight into the solvent behaviour across the ridges in both orientations, as illustrated in Figure 3. For a parallel-oriented fingerprint (i.e. the fingerprint lies parallel to the sampling path), the DESI solvent flows along the furrows before exiting the print (Figure 3Ai, Aii). This process is evidenced by

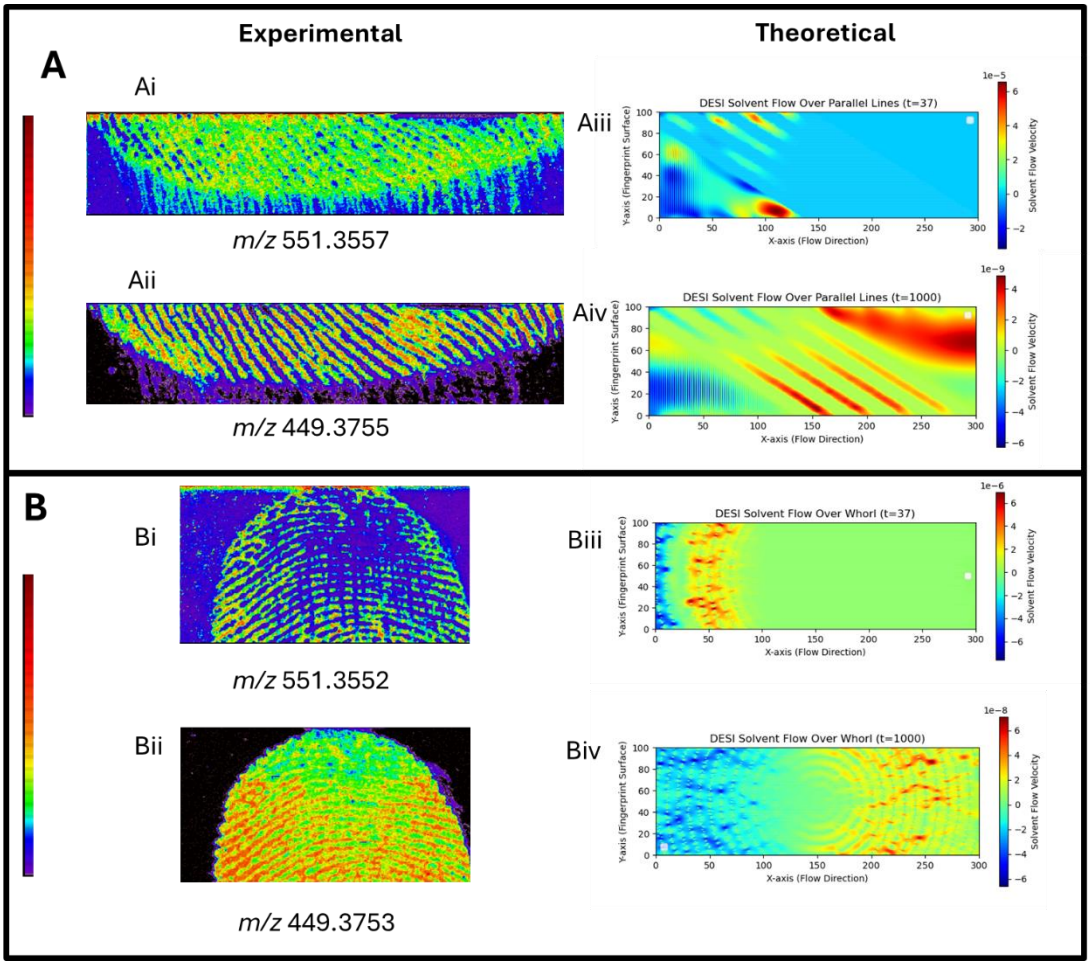

Figure 3. Variation of the bleeding effect with the fingerprint orientation for DESI-MSI. (A) showing the experimental and theoretical results for the parallel orientation of the fingerprint with ion images at (Ai) *m/z* 551.3557, (Aii) *m/z* 449.3755 and simulation images at (Aiii) t=37, (Aiv) t=1000. (B) showing the experimental and theoretical results for the perpendicular orientation of the fingerprint with ion images at (Bi) *m/z* 551.3552, (Bii) *m/z* 449.3755 and simulation images at (Biii) t=37, (Biv) t=1000. Imaging data are normalised by TIC. Pixel size at 50 µm.

the ion images at *m/z* 551.3557 and *m/z* 499.3755, which were selected to illustrate different degrees of movement, likely linked to their affinity for the molecular composition of the ridges and solubility in the DESI solvent. Our CFD model corroborates this mechanism, showing solvent transport along the simulated ridge lines at different simulation time steps of t=37 (Fig 3Aiii) and final step at t=1000 (Fig 3Aiv). The simulation is also shown as a video in Supplementary Video SV1. In contrast, for a perpendicular-oriented print (i.e. the fingerprint lies perpendicular to the sampling path (Figure 3B), both the experimental data and the CFD model show that this orientation causes the solvent to accumulate on the ridges before "spilling over" them and/or channelling through the natural gaps in the ridge continuity. This is observed in Fig 3Bi, through the ion image at *m/z* 551.3552, showing the

points of excess analyte accumulation and the subsequent spilling over of the solvent with the analyte. This "spillover" effect is significantly more detrimental to the fingerprint's integrity and, ultimately, to the quality of the biometric information. The resulting analyte deposition in the furrows could obscure key *minutiae* required for fingerprint identification, as observed in Fig 3Bii, where the ion image at *m/z* 499.3753 shows a "washed up" fingerprint due to the analyte flowing over the ridges, although portions of the fingerprints are still viable for *minutiae* recovery. The CFM model explains this phenomenon in detail, although it does not correlate to chemical composition or structure, where the solvent can be seen accumulating over some of the ridges trying to find a path to flow over (Fig 3Biii) at a time step of t=37. The spilling over of the solvent and its path through the fingerprint ridges can be clearly seen in the simulation at the final time step (t=1000) in Fig 3Biv. The simulation is also shown as a video in Supplementary Video SV2.

Consequently, for a DESI-MSI analysis of unenhanced latent fingerprints, as observed multiple times, a parallel sample orientation is preferred for the preservation of these crucial biometric features. This requirement brings up a first operational challenge for molecular fingerprinting by DESI-MSI in that, the achievement of optimal fingerprint image clarity and preservation of the original ridge pattern, requires the mass spectrometrist to correctly orientate each sample, a step that introduces variability, adds time to the analytical workflow and, most importantly, may not be visually possible for under-developed fingerprints. These requirement/challenges are not encountered in molecular fingerprinting via MALDI-MSI as: (i) post-matrix application, the uniform laser rastering makes sample orientation irrelevant, (ii) the integrity of the ridge pattern (and hence the resulting likelihood to obtain as many *minutiae* as possible, where present) are not at risk, if the matrix spraying conditions have been optimised to avoid analyte delocalisation.

DESI Imaging of Drug Contaminated Fingerprints

To evaluate the applicability of DESI-MSI for chemical intelligence associated with the biometric information, as well as to explore molecular bleeding further, with known analytes, drug-contaminated fingerprints were imaged and the bleeding effect assessed in each case. Building upon recent work that successfully imaged risperidone and its metabolite in fingerprints [28] in a multi-modal workflow, three additional antipsychotics were considered, namely olanzapine, alprazolam, and flunitrazepam. These drugs were selected to span a range of lipophilicity, following on the hypothesis that more lipophilic analytes are affected less by molecular bleeding, due to their affinity with the lipid molecular make-up of the ridges. As shown in Figure 4A, olanzapine ($C_{17}H_{20}N_4S$) was successfully imaged at *m/z* 313.1489 (+0.638 ppm) in a natural fingerprint contaminated using 50 µg of the drug deposited on a glass slide. Similarly, alprazolam ($C_{17}H_{13}ClN_4$) at *m/z* 309.0901 (-1.617 ppm) and flunitrazepam ($C_{16}H_{12}FN_3O_3$) at *m/z* 314.0944 (+1.273 ppm) were imaged at the same concentration (Fig 4 B,C). Considering the fingerprint area of ~273.9 mm^2 and the concentration and volume of the drugs employed being 1 mg/mL in 50 µL, olanzapine, alprazolam and flunitrazepam have been visualized at an over-estimated density

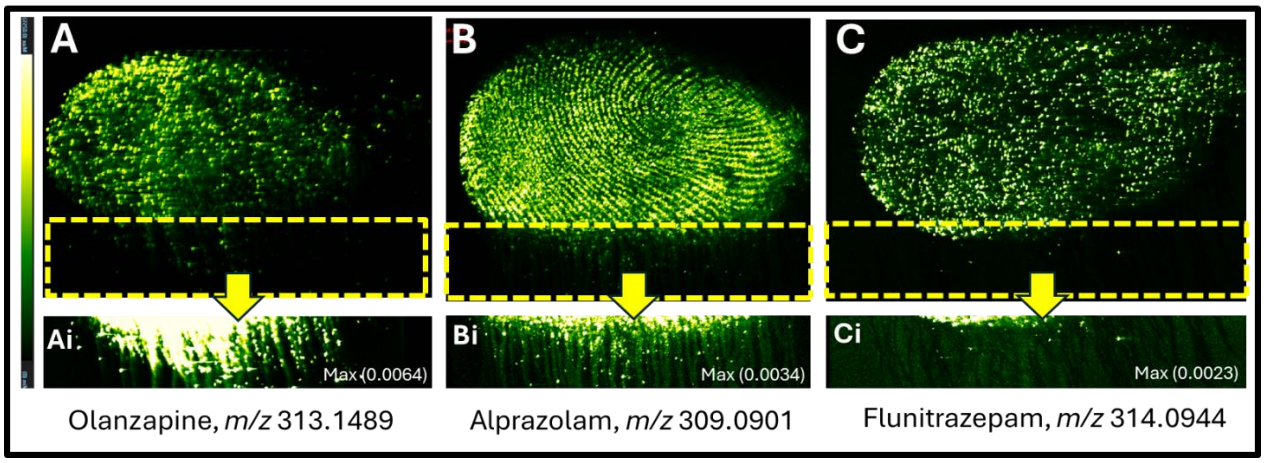

Figure 4. DESI-MSI of drug- contaminated fingerprints (with 50 µg of the drug deposited on the slide). (A) shows the ion image of olanzapine at *m/z* 313.1489, with the bleeding effect visualised at reduced intensity threshold (Ai). (B) shows the ion image of alprazolam at *m/z* 309.0901, with the bleeding effect visualised at increased intensity threshold (Bi). (C) shows the ion image of flunitrazepam at *m/z* 314.0944, with the bleeding effect visualised at reduced intensity threshold (Ci). Imaging data are normalised by TIC. Pixel size at 50 µm.

of <~182.5 ng/mm^2. We hypothesize that these imaging differences are driven by the interplay between the drug's lipophilicity and the DESI solvent and potentially, at a lower level, by the individual drug ionisation efficiency. Olanzapine appears to have a stronger affinity for the lipid-rich fingerprint ridges, resulting in an ion image which does not allow visualisation of the ridge flow and of the *minutiae* due to the potential partitioning of the analyte between the fingerprint and the DESI solvent. However, this affinity was not strong enough to avoid the bleeding effect as it can be seen in Fig 4Ai. Alprazolam yields a "cleaner" ion image at *m/z* 309.0901 with well-defined ridge details and moderate bleeding being observed (Fig 4Bi). Finally, flunitrazepam at *m/z* 314.0944, was likely susceptible to analyte delocalization through bleeding. This led to an image with poor ridge continuity, where the signal appears concentrated in lipid-rich pore locations (Fig. 4C). However, the analyte migration/delocalisation shows to be significantly reduced; this is not because of the absence of this effect but because of the significant washing away of the analyte (possibly due to higher solubility in the solvent) causing the drug presence to fall below the instrumental limit of detection. (Fig. 4 Ci). In an operational context, these observations imply that, whilst DESI MSI is broadly suitable for molecular fingerprinting and can efficiently yield useful chemical information from a fingerprint, from endogenous species to drugs of forensic relevance, (i) the "correct activity level proposition" may not be, eventually, indicated; indeed the drug presence in the furrows and in the area outside the fingerprint does not allow to infer whether the drug was already on the surface and not carried by the fingertip or transferred by a drug-contaminated fingertip; (ii) the extent to which DESI-MSI can produce a molecular map of a forensically relevant substance depicting

high quality/suspect identifying ridge detail is (apart from the common differences in ionizability of various molecules), speculatively, intrinsically linked to the compound's solubility in the DESI solvent and to its affinity with lipidic content of the ridges, and (iii) in the case of overlapping fingermarks where only one carries the forensically relevant substance, the bleeding effect may not allow to correctly ascertain which donor is the carrier. It must be pointed out that high concentration of the drugs (1 mgL/mL), more than adequately reflects a handling (touch chemistry) scenario (50 µg). However, it would not be representative of a "consumption" scenario and this may appear to be a limitation of the study. However, this concentration was selected deliberately to ensure a clear observation of the phenomenon, avoiding the risk of lack of detection or failure to generate an image due to much lower amounts spread across the fingermark area.

Effect of surfaces of deposition in Molecular Fingerprinting by DESI-MSI

Four surfaces of deposition have been selected for to investigate DESI-MSI performance in molecular fingerprinting namely glass, paper, tape lift, and gelatine lift. These surfaces are representative of non-porous, porous and semi-porous surfaces as well as the first two being common substrates on which fingermarks are found and the latter two being one of the means with which fingerprints are recovered from surfaces. Fingerprints were generated from the same fingertip but were imaged separately to maintain the exact spatial orientation to capture any instances of delocalisation, and also due to the inverted appearance of the lifted prints in the case of tape and gelatine lifts. Ion images collected from each surface, were selected to be representative, across the mass range, of the highest ridge pattern coverage/quality and are shown in Figure 5.

As general observation, the deposition surface may exert different levels of ion suppression or could have higher affinity for certain analytes making their ionisation more challenging. Therefore surfaces of deposition ultimately impact on the ions that could be detected or detected in a way that enables a "viable" fingermark image to be generated. This is why only the ion at nominal *m/z* 427 could be reported in Fig 5 as being in common between a fingermark on glass and one on paper. Optimised DESI-MSI acquisition parameters were applied to a latent mark deposited on the glass slide (representative of non-porous surface). Significant delocalisation was observed and two representative ions at *m/z* 427.3987 and *m/z* 610.5848 are presented (Figure 5 A,B). When a porous 100 GSM paper was used as representative of a porous substrate, delocalisation did not occur and we speculate that this can be ascribed to the paper's absorptive nature; however, ridge clarity was compromised by the radial diffusion (wicking) of analytes into the paper fibers, resulting in blurred ion images as representative ion images at *m/z* 427.3968 and *m/z* 481.3484 show (Figure 5C,D).

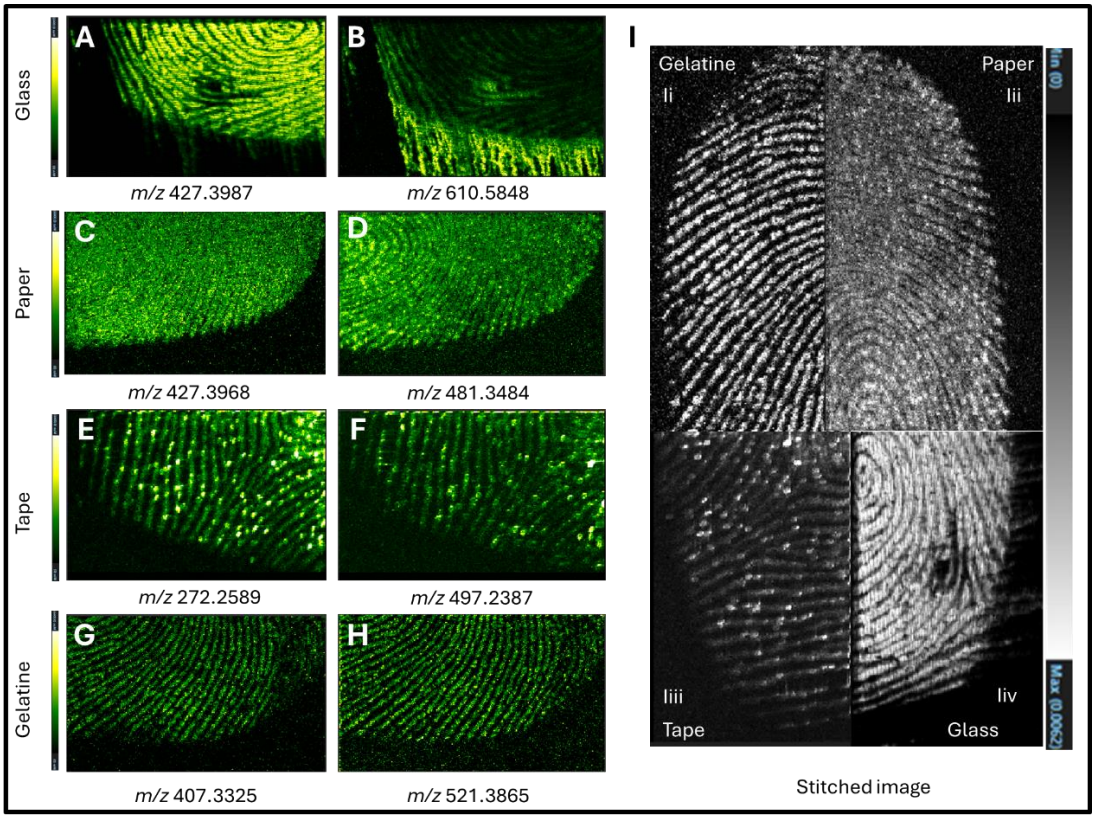

Figure 5. DESI-MSI of fingerprints on various forensically relevant surfaces. (A,B) ion images at *m/z* 427.3987 and *m/z* 610.5848 from a fingerprint deposited on glass. (C,D) ion images at *m/z* 427.3968 and *m/z* 481.3484 from a fingerprint deposited on paper. (E,F ion images at *m/z* 272.2589, and *m/z* 497.2387 from a fingerprint lifted from a black tile using a tape lift. (G, H) ion images at *m/z* 407.3325 and *m/z* 521.3865 from a fingerprint lifted from a black tile using a gelatine lifter. (I) stitched ion images from the 4 surfaces shown for comparison purposes; in particular (Ii) shows overlay images of ions at *m/z* 407.3325, *m/z* 521.3865, *m/z* 669.4980, and *m/z* 697.5306 from the gelatine lifter images; (Iii) shows overlay image of ion at *m/z* 481.3484 from the fingerprint on paper; (Iiii) shows images overlay of ions at *m/z* 272.2589, 449.3604 and *m/z* 497.2387 from the tape lift and (Iiv) shows images overlay of ion at *m/z* 427.3987 and m/z 409.3883 from a fingerprint deposited on glass. Imaging data are normalised by TIC. Pixel size at 50 µm.

This is consistent with our previous findings around the comparison between DESI and MALDI-MSI for risperidone/paliperidone- contaminated fingermarks on red paper enhanced with DMAC; in that instance, ridge merging and wicking of the analytes were observed, leading to poorer DESI images, in comparison with the MALDI images [28]. Similar results can be observed in the DESI images of Oil Red O (ORO) developed fingerprints on paper [31].

Tape and gelatine lifters were evaluated next after fingerprint enhancement with aluminium powder. Lifting tape proved to be a very poor substrate for DESI analysis likely due to the readily ionized compounds belonging to the adhesive side causing significant ion suppression of fingerprint analytes. This resulted in high chemical background images

obscuring both ridge detail and any potential bleeding. Importantly, the imaging analysis only produced three ridge forming ion images but those too at a low signal intensity. The ridge forming ion images at *m/z* 272.2589, and *m/z* 497.2387 are presented in Figure 5 E,F. Gelatine lifters were far more compatible, yielding much better ion image quality as shown for representative ions at *m/z* 407.3325 and *m/z* 521.3865 (Figure 5 G,H) aligning to recent work published by Frisch et al on gelatine lifted fingerprints imaged by DESI-MSI [24]. However, though the gelatine lifters enabled good quality images, there still was "chemical noise" in the image background. Frisch and team had used a DESI XS on the Waters Xevo G2-XS QToF with the Waters intelligent data capture (IDC) [43] was used by setting the high noise reduction function at 10 a.u (high value). This could possibly be the reason for the "cleaner" fingerprint images obtained in their study.

Here, the choice of fingerprint substrate highlights a key operational trade-off. The major advantage of DESI-MSI is its ambient nature, making it uniquely compatible with substrates that are problematic for MALDI's high-vacuum requirements, most notably high-moisture gelatine lifters. The data from the gelatine lifter show good quality ridge detail, with very little delocalisation detected making DESI-MSI the prime technique for imaging of fingermarks recovered by gelatine lifters, which are therefore recommended for fingerprint recovery at crime scenes, if DESI MSI can potentially be used to enhance the quality of the biometric information. It must also be noted that the fingermarks on glass are likely to also be recovered by lifting and hence the choice of DESI-MSI vs MALDI-MSI would depend on whether gelatine or lifting tape is used. Finally, it may be possible that a more highly textured surface (“rougher”) would enable higher quality fingermark images than those observed with the paper used in this work. This is because rougher surfaces minimise the solvent "washing" effect in DESI (observed in smooth, non porous surfaces) in addition to the possibility of a better analyte retention through absorption.

DESI-MSI comparative analysis of Fingerprints and Biological Tissue (Liver)

In order to address the hypothesis that the observed effect is “sample-specific", a DESI-MSI analysis was performed by including in the same imaging area both a fingerprint and a liver tissue section. The analysis of a fingerprint placed adjacent to and above a liver tissue section reveals the impact of the delocalisation to the extent that analytes bled from the fingerprint, well into the liver section. Once again, to illustrate this phenomenon, occurring across the entire mass range investigated, ions at *m/z* 230.2505 and *m/z* 466.3778 have been representatively selected and clearly observed bleeding from their original fingerprint location through and around the liver tissue (Fig. 6A, B). Consistent with our findings from Fig. 3, the solvent front carrying these analytes forms discrete flow paths, with some pooling on the topside of the liver tissue (Fig. 6A) while the majority diverts around the tissue boundary (Fig 6B).

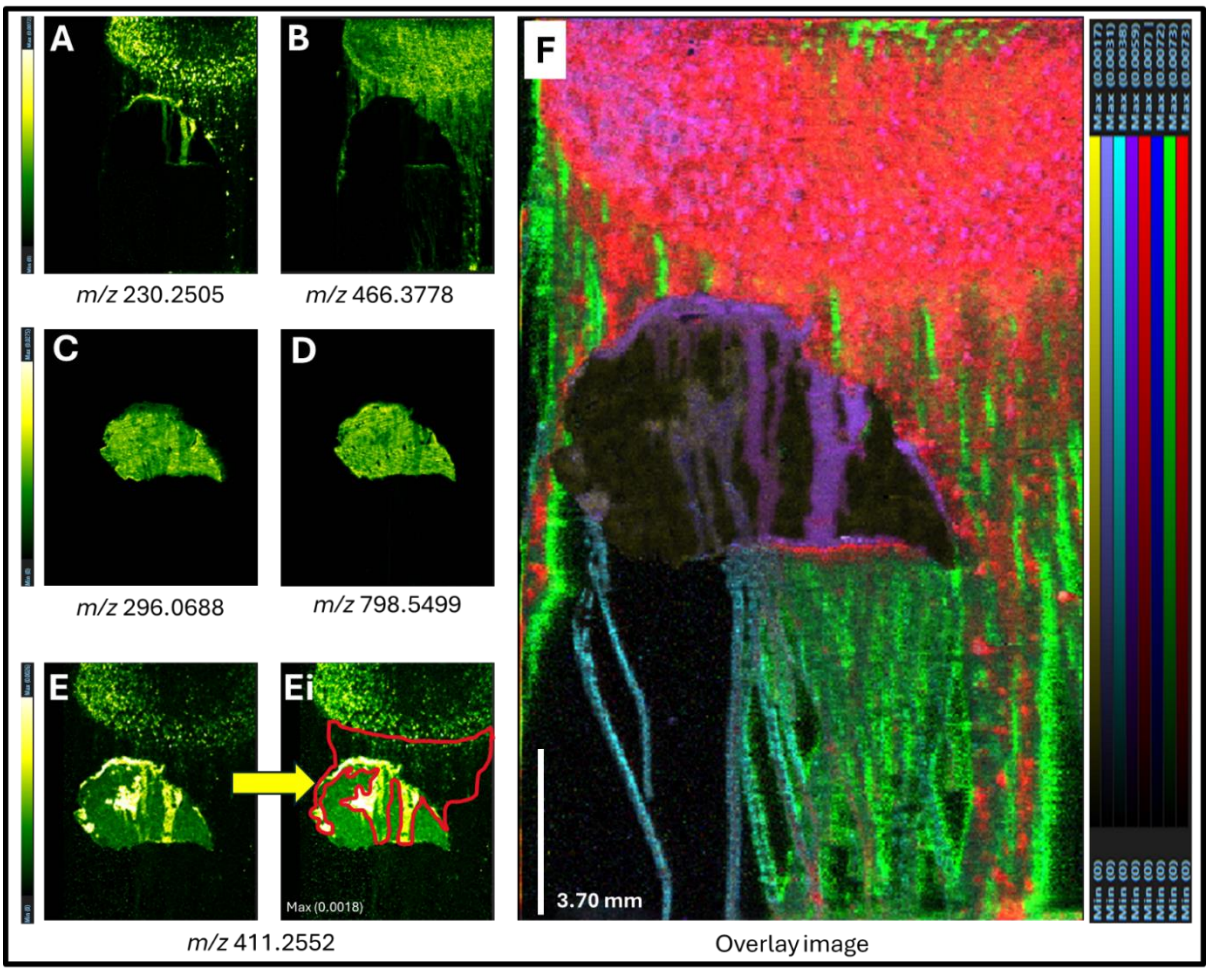

Figure 6. DESI-MSI analysis of a fingerprint and a liver section imaged in a single acquisition. (A,B) show representative ion at *m/z* 230.2505 and *m/z* 466.3778 from fingerprint. (C,D) show ion at *m/z* 296.0688 and *m/z* 789.5499 present in the liver representative of the absence of analyte delocalisation across the range investigated. (E) shows the image for a representative ion at *m/z* 411.2552 present in both the fingerprint and the liver with (Ei) showing an increased brightness image in which bleeding of the analyte from the fingerprint (highlighted in red) can be observed. (F) shows an overlayed image from ions at *m/z* 489.3233 (lavender), *m/z* 880.7650 (cyan), *m/z* 537.3615 (purple), *m/z* 466.3778 (Red), *m/z* 897.7434, *m/z* 530.3566 (green) and *m/z* 943.7209 (red) from fingerprints and at *m/z* 633.4942 (yellow) from the liver section. Imaging data are normalised by TIC. Pixel size at 50 µm.

In contrast, no ions originating from the liver tissue section were observed to migrate across and out the sample, as ions at *m/z* 296.0688 and *m/z* 798.5499 show (Figure 6C, D), selected as representative of the mass range investigated in the liver section and showing no delocalisation. This circumstance demonstrates the impact of a different sample, in this case the tissue section, in offering appropriate resistance to potential migration of analyte ions once the section is electrosprayed with the DESI solvent. To illustrate the bleeding

effect in a fair comparison, a representative ion, present both in the fingerprint and in the liver section, at *m/z* 411.2552, was selected to generate an image shown in Fig. 6E. Despite this ion is part of the molecular make up of both the fingerprint and the liver section, it migrates out of the fingerprint because of the bleeding effect, but it remains localised in the liver sample (Fig. 6Ei).

An overlay image (Fig. 6F) provides a comprehensive visualization of this phenomenon, highlighting the differential bleeding and different travel paths of various representative analytes at *m/z* 489.3233, *m/z* 880.7650, *m/z* 537.3615, *m/z* 466.3778, *m/z* 897.7434, *m/z* 530.3566, *m/z* 943.7209 as they migrate away from the fingerprint, transported by the DESI solvent through, and around the liver section. The same is shown in video format in Supplementary Video SV3).

This can pose a s problem in the DESI imaging of multiple unidentified fingerprint samples on a surface; there is in fact a possibility that the bleeding effect could lead to the analytes from one sample mixing with the other, thereby compromising both the attribution of the chemical intelligence and the provision of biometric information.

Multivariate analysis (PCA) was performed by extracting 5 ROIs from the fingerprint (FP), and liver to show a clear molecular make up based separation as expected (Fig 7A) with a PC1 variance of 96%. To understand the origin of the analytes, present in the bleeding area, in a second PCA analysis, 5 ROIs were extracted from the fingerprint (FP), the bleeding area between the fingerprint and the liver (BL1), the liver (L), and the bleeding area observed below the liver sample (BL2) as shown in Fig. 7B.

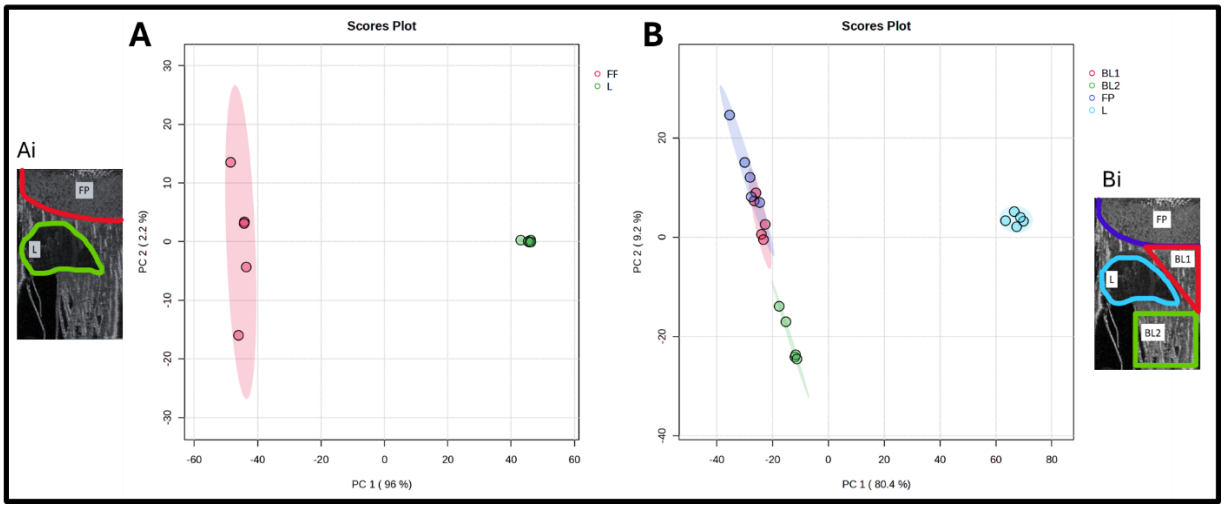

Figure 7. The principal component analysis (PCA) results. (A) Fingerprint (FP) and liver (L) section- 5 ROIs each selected from the regions denoted in the reference image (Ai). (B) Fingerprint (FP), bleeding area between fingerprint and liver section (BL1), liver (L), and the bleeding area after the liver section (BL2), with 5 ROIs each selected from the regions denoted in the reference image (Bi).

The PCA plot demonstrates clear molecular composition difference: the liver chemical composition is very different from that of the bleeding areas and fingerprint (PC1, 80.4% variance). While the bleeding areas (BL1/BL2) and fingerprint show compositional similarities, the scores form clusters, suggest a non-liver origin for the analytes in bleeding area.

In conclusion, based on the data presented in this study, DESI-MSI presents an attractive, sample preparation free and ambient alternative for fingerprint imaging, and the only solution to imaging fingerprints on gelatine lifters. However, its operational applicability to fingerprints in forensic casework may potentially be limited, presently, by challenges rooted in the technique's fundamental mechanism. It is important to note that while all the data presented in this work have been obtained after considerable optimisation, there is still scope for a further, more systematic and multi-variable-based study which could significantly and suitably minimise the bleeding effect.
In the authors' opinion, this effect may potentially be resolved by using nanospray desorption electrospray ionization (nano-DESI), which employs a liquid extraction-based probe that creates a dynamic liquid bridge on the sample surface [44].

Conclusion

As a direct DESI-MSI/MALDI-MSI comparison in the area of forensic molecular fingerprinting was not made in this study (and it will be the subject of follow up work), this paper has solely focussed on the *currently* observed advantages and *current* limitations of DESI MSI for molecular fingerprinting. We have confirmed the ability of DESI-MSI to provide excellent image quality, suitable for suspect identification, from fingerprints on gelatine lifters. This is crucial from an operational perspective as, whilst gelatine lifters are often used by Crime Scene Investigators, alongside tape lifts, to recover fingerprints, they cannot be analysed by vacuum MALDI-MSI due to the excessive water content of these substrates. We have also shown, for the first time, the potential challenge that DESI-MSI introduces in the provision of the biometric information with other fingerprint recovery means or surfaces of deposition. In particular, the delocalisation of analytes migrating from the ridges, through the ridges and pooling/flowing in the furrows, impacts the quality of the fingerprint images to various extents, depending on the orientation of the fingerprint with respect to the DESI solvent flowing path. In extreme delocalisation circumstances, this may compromise source attribution of the recoverable chemical intelligence, posing the question "did the presence of this forensically relevant substance originate from the fingerprint or the surface of deposition?"
Within the present study, the negative impact on the recovery of the *minutiae* and ridge flow, may compromise suspect identification from 3 out of the 4 deposition surfaces investigated. However, importantly and generally, if even only one, out of all ion images

generated from any of those surfaces, contained viable ridge detail, then suspect identification may still be possible. Furthermore, there is still scope to investigate how to counteract and mitigate this effect with a further exploration of: (i) all the parameters/variables/settings in a cross talking fashion encompassing the full operational space of DESI MS, (ii) a higher number of surfaces of deposition and fingermark types, (iii) a direct comparison with MALDI-MSI on a large number of split marks to fully and accurately elucidate the limitations and advantages of DESI for molecular fingerprinting and (iv) inter-lab validation of fingermark DESI imaging.

In addition, it is conceivable to even intervene through engineering an auxiliary accessory to enable controlled and suitable solvent droplets evaporation to still allow formation of secondary droplets containing the analyte sample, whilst minimising excess solvent acting as analyte transporter through the fingerprint sample. It is also important to remember, that the bleeding effect has only been observed so far for fingerprint samples, which is a niche imaging application, as opposed to the mainstream tissue imaging applications.

Altogether, in the area of molecular fingerprinting this paper strongly suggests that there is a justified drive and reasonable grounds to support the need for a systematic study to explore in more depth how the current bleeding effect observed in DESI MSI of fingerprints can be suitably reduced or eliminated.

Supporting Information

Additional literature and experimental details information include an histogram chart for the former, a experimental parameters/settings for the latter as well as supporting videos and figures.

Acknowledgments

The authors are grateful for the PhD studentship funding to Rohith Krishna jointly awarded by Sheffield Hallam University and Waters Corporation. The authors also wish to acknowledge Dr James Langridge and Dr Emmanuelle Claude from Waters Corporation for the several constructive and critical discussions around DESI-MSI optimisation for fingermark imaging.

References

1. Francese, S.; Bradshaw, R.; Denison, N. An Update on MALDI Mass Spectrometry-Based Technology for the Analysis of Fingermarks—Stepping into Operational Deployment, *Analyst* **2017**, *142*, 2518–2546

2. Bailey, M. J.; Bradshaw, R.; Francese, S.; Salter, T. L.; Costa, C.; Ismail, M.; Webb, R. P.; Bosman, I.; Wolff, K.; de Puit, M. Rapid detection of cocaine, benzoylecgonine and methylecgonine in fingerprints using surface mass spectrometry, *Analyst* **2015**, 140 (19), 6254–6259

3. Bradshaw, R.; Denison, N.; Francese, S**.** Implementation of MALDI MS profiling and imaging methods for the analysis of real crime scene fingermarks, *Analyst* **2017,** *142* (9), 1581–1590

4. Ferguson, L. S.; Wulfert, F.; Wolstenholme, R.; Fonville, J. M.; Clench, M. R.; Carolan, V. A.; Francese, S. Direct detection of peptides and small proteins in fingermarks and determination of sex by MALDI mass spectrometry profiling, *Analyst* **2012**, *137* (20), 4686–4692

5. Heaton, C.; Bury, C. S.; Patel, E.; Bradshaw, R.; Wulfert, F.; Heeren, R. M.; Cole, L.; Marchant, L.; Denison, N.; McColm, R.; Francese, S. Investigating sex determination through MALDI MS analysis of peptides and proteins in natural fingermarks through comprehensive statistical modelling, *Forensic* Chem. 2020, 20, 100271

6. Heaton, C.; Witt, M.; Cole, L.; Eyre, J.; Tazzyman, S.; McColm, R.; Francese, S. Detection and mapping of haemoglobin variants in blood fingermarks by MALDI MS for suspect "profiling", *Analyst* **2021**, 146 (13), 4290–4302

7. Bradshaw, R.; Wolstenholme, R.; Ferguson, L. S.; Sammon, C.; Mader, K.; Claude, E.; Blackledge, R. D.; Clench, M. R.; Francese, S. Spectroscopic imaging based approach for condom identification in condom contaminated fingermarks, *Analyst* **2013**, *138* (9), 2546–2557

8. Kaplan-Sandquist, K.; LeBeau, M. A.; Miller, M. L. Chemical analysis of pharmaceuticals and explosives in fingermarks using matrix-assisted laser desorption ionization/time-of-flight mass spectrometry *Forensic Sci. Int.* **2014**, *235*, 68–77

9. Longo, C. M.; Musah, R. A. MALDI-Mass Spectrometry Imaging for Touch Chemistry Biometric Analysis: Establishment of Exposure to Nitroaromatic Explosives Through Chemical Imaging of Latent Fingermarks, *Forensic Chem.* **2020**, *20*, 100269

10. Rowell, F.; Hudson, K.; Seviour, J. Detection of drugs and their metabolites in dusted latent fingermarks by mass spectrometry *Analyst***, 2009,**134**, 701-707**

11. Wolstenholme, R.; Bradshaw, R.; Clench, M. R.; Francese, S. Study of latent fingermarks by matrix-assisted laser desorption/ionisation mass spectrometry imaging of endogenous lipids *Rapid Commun. Mass Spectrom.* **2009**, *23* (19), 3031–3039

12 Francese, S.; Heaton, C. Emerging Technologies: Use of Matrix Assisted Laser Desorption Ionisation Mass Spectrometry for the Analysis of Fingermark and Blood Evidence. In *Applications of Mass Spectrometry for the Provision of Forensic Intelligence: State-of-the-Art and Perspectives*; Francese, S., Bleay, S. M., Eds.; Royal Society of Chemistry: 2023; pp 159–183. ISBN: 978-1-83767-193-9.

13. Bandey, H., Ed. *Fingermark Visualisation Manual*; Home Office Centre for Applied Science and Technology (CAST): Sandridge, UK, 2014.

14. Bandey, H., Ed. *Fingermark Visualisation Manual*, 2nd ed.; Defence Science and Technology Laboratory (Dstl): 2022; ISBN 978-1-3999-0976-1.

15. Ifa, D. R.; Manicke, N. E.; Dill, A. L.; Cooks, R. G. Latent fingerprint chemical imaging by mass spectrometry *Science* 2008,*321* (5890), 805.

16. Cooks, R. G.; Ouyang, Z.; Takáts, Z.; Wiseman, J. M. Ambient Mass Spectrometry. *Science* **2004**, *306* (5695), 471–473F

17. Takáts, Z.; Strittmatter, N.; McKenzie, J. S. Ambient Mass Spectrometry in Cancer Research. In *Advances in Cancer Research*; Drake, R. R., McDonnell, L. A., Eds.; Academic Press: 2017; Vol. 134, pp 231–256. ISBN 978-0-12-805249-5.

18. Brown, H. M.; Alfaro, C. M.; Pirro, V.; Dey, M.; Hattab, E. M.; Cohen-Gadol, A. A.; Cooks, R. G**.** *J. Appl. Lab. Med. 2021, 6 (4), 902–916*

19. Seidinger, A. L.; Silva, F. L. T.; Euzébio, M. F.; Krieger, A. C.; Meidanis, J.; Gutierrez, J. M.; Bezerra, T. M. S.; Queiroz, L.; Silva, A. A. R.; Hoffmann, I. L.; Daiggi, C. M. M.; Tedeschi, H.; Eberlin, M. N.; Eberlin, L. S.; Yunes, J. A.; Porcari, A. M.; Cardinalli, I. A. Tumor-Promoted Changes in Pediatric Brain Histology Can Be Distinguished from Normal Parenchyma by Desorption Electrospray Ionization Mass Spectrometry Imaging *Biomedicines* **2024**, *12* (11), 2593

20. Bardin, E.; Claude, E.; Takáts, Z. Analysis of Fingerprints by Desorption Electrospray Ionization Mass Spectrometry Imaging Application Note No. 720005884; Waters Corporation & Imperial College: 2018

21. Shi, J.-W.; Zheng, L.-N.; Ma, R.-L.; Wang, B.; Chen, H.-Q.; Wang, M.; Wang, H.-F.; Feng, W.-Y. Chemical Analysis and Imaging of Fingerprints by Air-flow Assisted Desorption Electrospray Ionization Mass Spectrometry *Chinese J. Anal. Chem.* **2019**, *47* (12), 1909–1914

22. Carrà, A.; Falciola, L.; Cappelletti, G.; Morosi, L.; Davoli, E. Chemical Images on Fingerprints Revealed with Mass Spectrometry *Appl. Sci.* **2021**, *11*, 5624

23. Costa, C.; Jang, M.; de Jesus, J.; Steven, R. T.; Nikula, C. J.; Elia, E.; Bunch, J.; Bellew, A. T.; Watts, J. F.; Hinder, S.; Bailey, M. J**.** Imaging mass spectrometry: a new way to distinguish dermal contact from administration of cocaine, using a single fingerprint *Analyst* **2021**, *146* (12), 4010–4021

24. Frisch, K.; Nielsen, K.L.; Hasselstrøm, Jo.B.; Fink, R.; Rasmussen, S.V.; Johannsen, M. Desorption Electrospray Ionization Mass Spectrometry Imaging of Powder-Treated Fingermarks on Forensic Gelatin Lifters and its Application for Separating Overlapping Fingermarks *Analytical Chem.* **2024,** 96, 12497-12507

25. Mirabelli MF, Chramow A, Cabral EC, Ifa DR. Analysis of sexual assault evidence by desorption electrospray ionization mass *spectrometry J Mass Spectrom*. **2013**, 48, 774-778

26. Helmond, W. V.; Begieneman, M. P. V.; Kniest, R.; Puit, M. Classification of condom lubricants in cyanoacrylate treated fingerprints by desorption electrospray ionization mass spectrometry *Forensic Sci. Int*. **2019**, 305, 110005

27. Rajs, N.; Harush-Brosh, Y.; Raisch, R.; Yakobi Arancibia, R.; Zoabi, A.; Golan, G. N.; Shpitzen, M.; Wiesner, S.; Levin-Elad, M.; Kaplan, T.; Margulis, K. Determining time since deposition of latent fingerprints on forensic adhesive tape using ultrafast DESI-MS and machine learning *Sci. Rep.* **2025**, *15*, 18413

28. Krishna, R.; Hamer, K.; Bradshaw, R.; Bleay, S.; Cole, L. M.; Claude, E.; Langridge, J.; Buček, J.; Francese, S. A multi-modal mass spectrometry approach for the detection and mapping of date **rape** *drugs in fingermarks* Analyst *2025,* 150*,* 2498–2513

29. Muramoto, S.; Forbes, T. P.; van Asten, A. C.; Gillen, G. Test Sample for the Spatially Resolved Quantification of Illicit Drugs on Fingerprints Using Imaging Mass Spectrometry *Anal. Chem.* **2015**, *87*, 5444–5450

30. Zhou, Z.; Zare, R. N. Personal Information from Latent Fingerprints Using Desorption Electrospray Ionization Mass Spectrometry and Machine Learnin g*Anal. Chem.* **2017**, 89, 1369−1372

31**.** Banidol, M.; Kouider, S.; Sergent, I.; Pizzala, H.; Charles, L**.** Desorption electrospray ionization mass spectrometry imaging of latent fingerprints revealed by Oil Red O *Rapid Commun. Mass Spectrom*. 2024, 38, e9724

32. Krishna, R.; Langridge, J.; Claude, E.; Bradshaw, R.; Cole, L.; Francese, S. Systematic Method Optimisation Approach for Small Molecule Imaging on the SELECT SERIES MALDI MRT-Drug Mapping in Fingerprints, a Case Study. Anal. Chim. Acta 2025, 1354.

33. Pang, Z.; Lu, Y.; Zhou, G.; Hui, F.; Xu, L.; Viau, C.; Spigelman, A.; MacDonald, P.; Wishart, D.; Li, S.; Xia, J. MetaboAnalyst 6.0: Towards a Unified Platform for Metabolomics Data Processing, Analysis and Interpretation. Nucleic Acids Res. 2024, 52, 398-406.

34. Groeneveld, G.; De Puit, M.; Bleay, S.; Bradshaw, R.; Francese, S. Detection and Mapping of Illicit Drugs and Their Metabolites in Fingermarks by MALDI MS and Compatibility with Forensic Techniques. *Sci. Rep.* **2015**, *5*), 11716.

35. Krüger, T.; Kusumaatmaja, H.; Kuzmin, A.; Shardt, O.; Silva, G.; Viggen, E. M. *The Lattice Boltzmann Method: Principles and Practice*; Springer International Publishing: Cham, Switzerland, **2017**.

36. Xu, K. A.; Generalized Bhatnagar–Gross–Krook Model for Nonequilibrium Flows. *Phys. Fluids* **2008**, *20,*2.

37. Khatami, A.; Prova, S.S.; Bagga, A.K.; Yan Chi Ting, M.; Brar, G.; Ifa, DR.; Detection and imaging of thermochromic ink compounds in erasable pens using desorption electrospray ionization mass spectrometry. Rapid Commun Mass Spectrom. **2017,** 31,, 983-990

38. Tibljas, V.; Francese, S.; Da Costa Abreu, M.; Bradshaw, R.; A multimodal mass spectrometry imaging workflow for ballpoint pen ink analysis and "forgery" detection. Analyst. **2025**, 150(11), 2322-2335

39. Tibljas, V.; Francese, S.; Clark, J.;, Goodall, I.; Birch, F.; Bradshaw, R.; Multimodal analytical approach applied to whisky labels for authenticity determination *Forensic Chemistry*, **2025**, *46*, 100709

40. Bandey, H.L., Fingerprint Development and Imaging Newsletter: The Powders Process, Study 1, Police Scientific Development Branch, Home Office, Sandridge, **2004**, Report No. 54/04.

41. Ramatowski , R.S. Composition of Latent Print Residue in Advances in Fingerprint Technology. CRC Press: Boca Raton, **2001**.

42. Gromnicka, D.; Wałecki, B. Usefulness of the analysis of the average ridge width of fingerprints in archaeological research. *Anthropological Review* **2022**, 85, 31–49.

43. Ranbaduge, N.; Yu, Y. Q. Intelligent Data Capture (IDC) Enables Optimal Xevo G2-XS Data Acquisition and Processing for Multi-Attribute Method (MAM) Studies. Waters Corporation, Application Note 720007441EN, 2021.

44. Roach, P. J.; Laskin, J.; Laskin, A. Nanospray Desorption Electrospray Ionization Mass Spectrometry. Analyst 2010, 135, 2233–2236. DOI: 10.1039/C0AN00312C.